DTU Library

Evaluation of the ID220 single photon avalanche diode for extended spectral range of photon time-of-flight spectroscopy

Nielsen, Otto Højager Attermann; Dahl, Anders Bjorholm; Anderson-Engels, Stefan; Nielsen, Frederik Donbæk; Thomsen, Carsten Lilholt; Khoptyar, Dmitry

Evaluation of the ID220 single photon avalanche diode for extended spectral range of photon time-of-flight spectroscopy

Otto H. A. Nielsen,* Ander Bjorholm Dahl, and Stefan Anderson-Engels

Department of Applied Mathematics and Computer Science, Technical University of Denmark, 2800 Kgs. Lyngby, Denmark

Frederik Donbæk Nielsen and Carsten Lilholt Thomsen

NKT Photonics A/S, Blokken 84, 3460 Birkerød, Denmark

Dmitry Khoptyar

Department of Physics, Lund University, P.O Box 118 S-221 00 Lund, Sweden

* Coresponding author: otni@dtu.dk

DTU Compute Technical Report-2014-06

ABSTRACT

This paper describe the performance of the ID220 single photon avalanche diode for single photon counting, and investigates its performance for photon time-of-flight (PToF) spectroscopy. At first this report will serve as a summary to the group for PToF spectroscopy at the Department of Physics, Lund University (Sweden) together with ID Quantique Inc. (Genève, Switzerland). As such, the report does not give an introduction to PToF spectroscopy, which may be found om the Doctoral on the topic [2, 3, 19]. The report focuses on a description of the detectors ability to measure the PToF distribution of infrared light.

First, a motivation for using the ID220 for measuring PToF distribution is given, followed by a brief description of the experimental setup in which the detector was characterized. Following this, the quantification of delay using cross correlation between PToF distributions is described. This allows the changes in delay and shape to be characterized. A technique for reducing measurement artefacts by lowering the repetition rate of the light source is also investigated. Lastly, the applicability of the detector for PTOF spectroscopy is discussed and conclusions drawn about its suitability for this application.

Version History

Version	Date	Change revision
1.0	15 / 7 / 2013	First summary of measurements
1.1	20 / 10 / 2013	Updated results section
1.2	11 / 1 / 2014	Included description of single photon avalanche diodes.

INTRODUCTION

The aim of this work is to investigate the suitability of a newly available single photon avalanche diode (SPAD) for near infrared PTOF spectroscopy. The use of such detectors has recently been reported by Pifferi *et al.* [18], however not all properties of these detectors have been addressed. In this report we focus on how the detector performance can be quantified using interpretable features (width and arrival time) which are important for any quantitative analysis of PTOF distributions. The characterization is first performed independently of our specific application, and as such it provides a general approach for SPAD characterization and an objective basis for identifying improvements to the devices.

The instrument has been investigated for PToF spectroscopy, a technique that allows deduction of the scattering and absorption properties of a material simultaneously. Using Lorenz-Mie theory, the scattering coefficients can be used to quantify a sample's structural composition in terms of particle size and shape distributions [8, 11, 20]. The absorption coefficient gives information on the sample's chemical constituents, because absorption arises from specific electronic and rotational-vibrational transitions in its atoms or molecules [6] A general introduction to the field of diffuseoptical spectroscopy is given by Martelli *et al.* [15]. The advantage of PToF spectroscopy is its ability to deduce optical properties without knowledge of the source power of the illumination. Instead, the change a short light pulse exhibits when passing through the sample is analyzed. The sample will delay the PToF together with broadening its temporal profile. Thus it is essential that the temporal delay of the pulses is measured with high accuracy and in an unbiased way. Similarly, the temporal width of the PToF distribution is influenced mainly by absorption, for measurements of which it is critical that the width be measured adequately.

The ID220 detector has been investigated as a replacement for a photon multiplier tube (PMT), that up until now has been used for the wavelength regime 900 - 1400 nm. PMT's require cooling by liquid nitrogen, operate at very high voltages, and are, in general, bulky. The advantage of using a solid state detector would be an extended spectral range, where measurements up to 1700 nm have been demonstrated [4], and the same range is covered by the ID200. The combined PToF spectroscopy setup would also benefit from a significantly to use, which would allow measurements in clinical facilities or during production in industry.

An illustration of the structure of a SPAD is shown in Figure 1(a). An introduction to the detector technology is given by Fishburn and Charbon [9]. In principle, the diode is a p-n junction operated in reverse bias, with the bias set to a level above the breakdown voltage. This form of operation is often referred to as the "Geiger mode". In this mode, the multiplication region can induce new cascades due to both electrons and holes. The cycle which the

(a)Structure of a SPAD as reported by Lunghi [13]

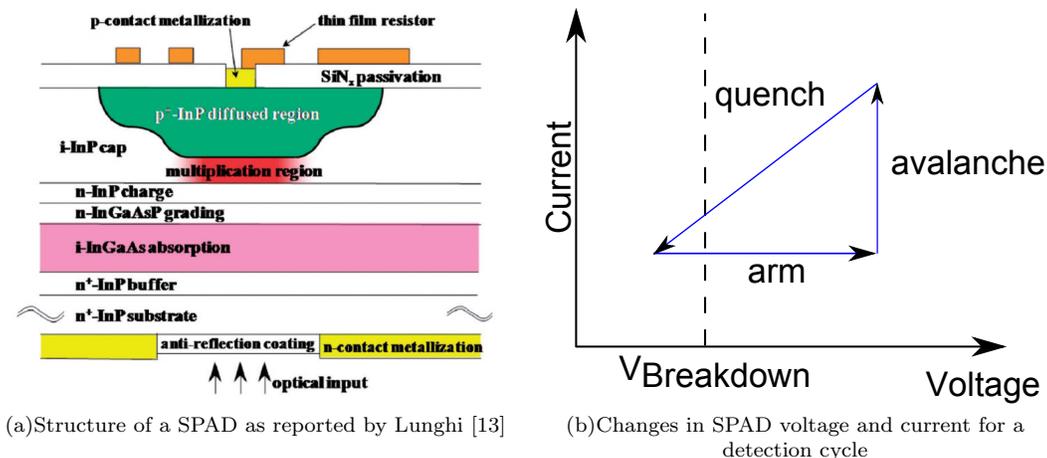(b)Changes in SPAD voltage and current for a detection cycle

Figure 1. Illustration of the structure of an SPAD and the principle of its operation.

detector undergoes in a detection process is illustrated in Figure 1(b). The starting mode is an "armed" state ot the lower right where the diode's voltage is set to a voltage exceeding the breakdown voltage. From here the detection of a photon causes an avalanche current in the diode, which is stopped by the "quenching" process. From here the voltage is reset and the cycle may repeat.

One of the limitations of the SPAD technology is afterpulsing of the detectors, which causes additional artificial detections when measuring the PToF distribution. These arise due to trapped electron-hole pairs which causes new avalanches after an actual detection event, hence the term after-pulsing. A physical interpretation of afterpulsing in SPAD detectors are given by Itzler *et al.* [10]. Suggestions for reducing afterpulsing while maintaining a high count rate are given in [4, 12, 16] which all employ gating of the detector signal to avoid artifacts. The ID220 uses a passive quenching technique, to reduce the non-linearity of the detector. The afterpulsing properties of the ID220 in particular have been investigated specifically in references [13, 21], but without investigating the pulse shape characteristics.

We present a characterization technique for the combined instrument, quantifying measurement perturbations independent of the source of error - whether afterpulsing, quenching or waveform generation.

EQUIPMENT AND DATA ACQUISITION

To quantify the instrument's performance with respect to estimation of both temporal delay and the width of the light pulses, it was combined with an instrument for PToF spectroscopy at NKT Photonics A/S (Birkerd, Denmark) in collaboration with Lund Photon time-of-flight spectroscopy laboratory. An illustration of the PToF spectrometer is presented in Figure 2.
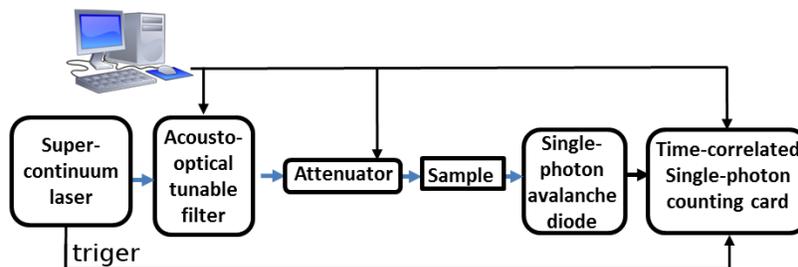

Figure 2. A schematic of the photon time-of-flight spectrometer. The black lines are electronic signals, and blue are optical.

The PToF spectrometer uses a supercontinuum light source (SuperK Extreme EXB-4). The laser operates at a repetition rate of 80 MHz, but a built-in pulse picker feature allows a selectable repetition rate in an interval between 2 - 80 MHz for the present source. The supercontinuum light is spectrally filtered using an acousto optical tunable filter (AOTF) with a SuperK SELECT (NKT Photonics - Birkerd Denmark). The system provide a temporally narrow laser pulse which can be tuned in the spectral range from approximately 400 nm - 2000 nm. The light pulses, filtered

by the AOTF are delivered by a fiber based delivery system (LMA-10 NKT Photonics) and propagate afterwards in gradient-index fibers with a 400 μm core (Leoni Fiber Optics, Germany). To obtain sufficiently low intensity levels to permit single photon counting, we perform an adjustable attenuation of the pulse intensity by a fibre coupled attenuator (DD-100, OZ Optics, Canada). These attenuators are integrated into the measurement routines that are used for data acquisition. The laser intensity is reduced by positioning either a sample for a thin piece of paper in the optical path as when operated for PToF spectroscopy. This also has the effect of exiting all the optical modes of the GRIN fibre. The light pulses are afterwards sent to the ID220 detector. To construct a PToF distribution the detector output is wired to a time correlated single photon count (TCSPC) module (SPC-130EM - Becker & Heckl - Germany). The seed pulse from the super continuum light source is used as a time reference for the TCSPC card.

The installation of the detector is as described in the application note [1], a 12 dB attenuation is used between TCP card and the ID220 however. The TCP card settings for constant fraction discriminator level and range were adjusted to avoid a double peak structure and similar artifacts during data acquisition. Unless otherwise noted, all measurements of the PToF distributions were made over 32 seconds to ensure a decent signal to noise performance.

Dead time and Quantum efficiency

The ID220 has two adjustable parameters, the dead time after detection and the quantum efficiency (QEF), the effect of these was explored prior to the instrument characterization. The dead time can take integer values in the range 1 - 20 μs, and the QEF can be set to 10, 15 and 20 %. One of the key difference between InGaAs based SPADs and silicon based SPAD's is the necessity of long dead times after detection to avoid afterpulsing. The effect of setting dead time and QEF was quantified in terms of the dark count rate, and the results are presented in Figure 3.
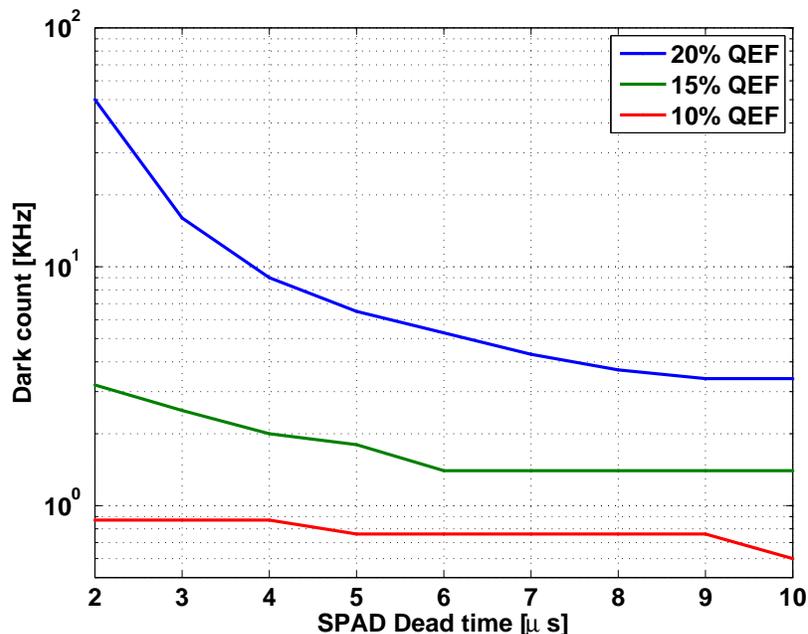

Figure 3. Measured dark counts as a function of dead time for different quantum efficiencies of the ID220.

Similarly the detector response time is dependent on the QEF, the TWHM values are summarized in table I.

QEF [%]	20	15	10
FWHM [ps]	154	218	487

Table I. Instrument response function vs. quantum efficiency.

From these measurements it may be seen that an increase in the dead time significantly reduces the number of dark counts. Similarly the dark counts are reduced significantly by a low QEF value. The specific value of the dead time which is suitable for our application could not be determined from the characteristics of the dark counts alone,

beacause although an increase in dark count rate adds noise to the PToF distribution, it will also allow a higher count rate.

The measured instrument response time shows a significant increase when operating with a QEF of less than 20 %, as is seen from table I. For this reason, it was decided to operate the device with a QEF of 20 % to obtain the highest possible time resolution. The instrument response of the combined setup without the additional broadening of the detector is expected to be 40 *ps* based on measurements with a silicon SPAD.

Quantifying instrument linearities

An application-independent assessment of the linearity of the system is performed by measuring the change in pulse width and arrival time of the light pulse. The shape change is quantified by calculating the FWHM of the profile and the delay is quantified by measuring the change in arrival time. To measure the latter part with high accuracy, the cross-correlation of the profile is calculated with a reference pulse and the location of the peak position is extracted from the autocorrelation. In practice a third degree polynomial is fitted to the peak intensity part of the autocorrelation and the apex of this is used. An example of this technique and the analysis is presented in Figure 4, the two signals which are compared are the two most extreme from the time series presented later in Figure 5, with a separation of 92 ps. For each measurement series the absolute value of the delay is always relative, the signal with highest count rate is used because this has the best signal to noise.
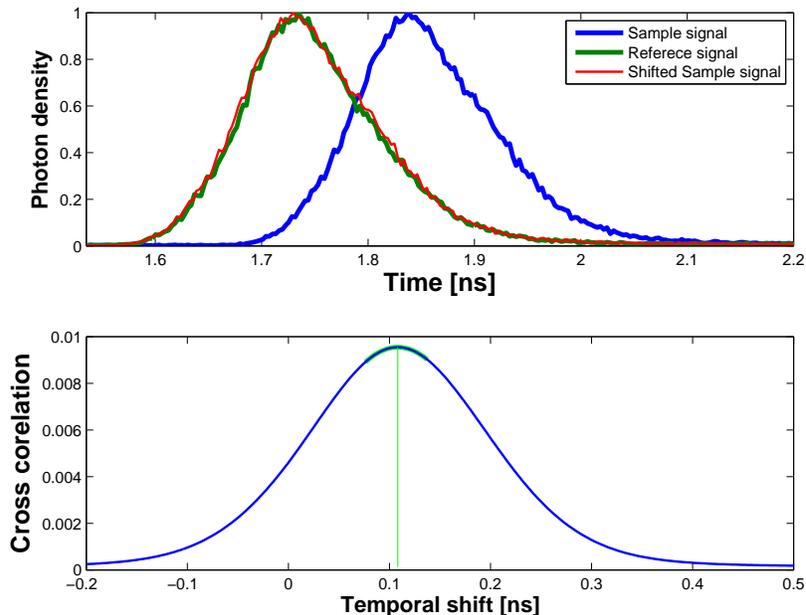

Figure 4. Example of how the temporal delay is calculated. **Top:** Examples of photon time-of-flight distributions and their overlap after using their cross correlation to estimating the temporal shift. **Bottom:** Cross correlation of the two profiles together with the fitted polynomial at the center. The position of the peak is marked with a vertical green line.

The results show that visually a perfect overlap between the two profiles is achieved, and the shape of the cross correlation suggests that the noise in the estimation is very small.

Intrinsic fluctuation of the light source

To estimate precision and any possible intrinsic variation in the PToF distribution arising from the combined setup, the PToF distribution was recorded for $\sim$ 70 hours, at 1510 nm, and the delay and FWHM were calculated. The results are presented in Figure 5. The attenuation was fixed during measurement and a total count rate of 4.40 kHz ± 0.13 kHz with a detector dead time of 10 μs was used. The PToF distribution is recorded by triggering the clock on the TCP card by the first stage in the light generation process (the seed pulse). This signal pulse is thus not necessarily synchronized with the optical output of the laser.
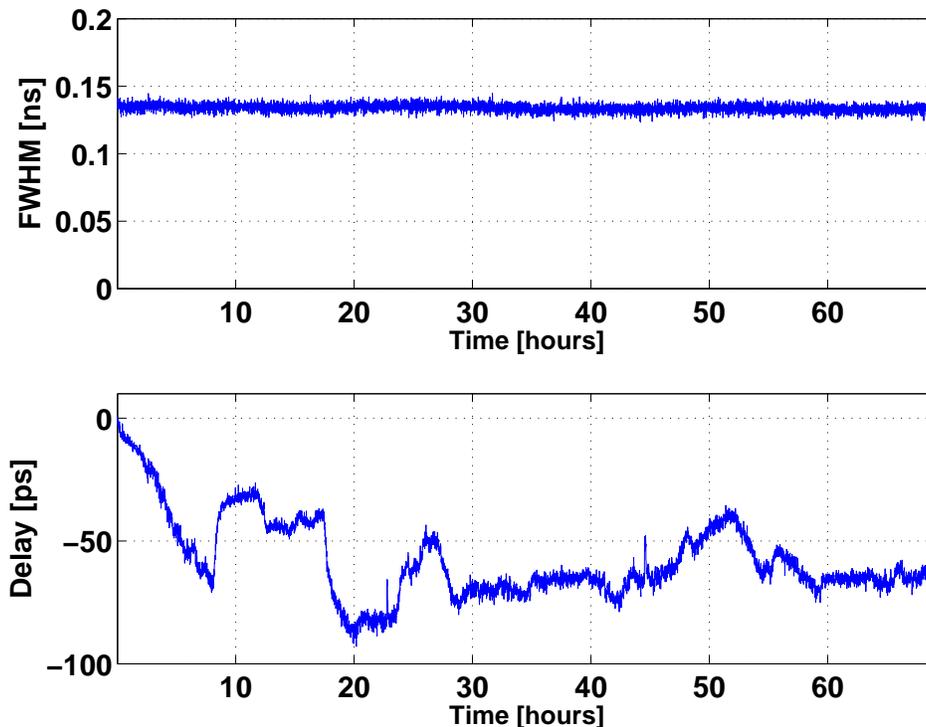
Figure 5. Time stability of the light source. **Top:** Measured full width half maximum of the PToF distribution. **Bottom:** Measured delay compared to the start point.

The results show that the FWHM is very constant throughout the measurement. This shows that the temporal profile of the light pulse is unchanged during operation. The delay however varies a little over time, and is estimated with a precision of ~ 5 ps as this is the variance on short time scales, the accuracy will depend on the ratio of signal to noise in the PToF distribution. For this reason repetitive measurements are performed during analysis later on to estimate precision at each measurement point. The variation on longer time scales is approximately ~ 25 ps. This long term drift can be avoided by triggering on the actual output from the light source, but this is outside the scope of the present work.

The measurements serve as a validation of the analysis of both the light pulses arrival time and shape. Though only measured at a single wavelength, we suspect this to be a general result. The mechanism that drives the super continuum generation locks the average position of the different wavelengths in a well defined pattern [7]. Scatter plots, not shown here, of the correlation between the measured count rate and the delay and FWHM respectively revealed no correlation.

ID220 INSTRUMENT RESPONSE FUNCTION

As explained previously it is imperative for PToF spectroscopy that the light pulse is characterized without artifacts. In single photon counting the count rate is arbitrary, but should be set low enough to avoid perturbation of the profile and the integration time should be sufficient to ensure a good signal to noise level. In this section we investigate how the delay and FWHM of the instrument change with count rate.

The PToF distribution of an optical phantom is presented in the left column of Figure 6 for different count rates. The pulse width and delay relative to the lowest noise signal, measured at 95 kKHz is calculated and presented in the right column of Figure 6. The optical phantom is composed by a combination of a pulverized BG36 bandpas filter and a expoxy plastic. The phantom is 1.9 mm thickness and was measured with a wavelength of 1000 nm. The detector was operated with a QEF of 20 % and a dead time of 10 μs.

A first observation was that by setting the CFD values for the TCP card properly it is possible to measure PToF distributions without additional peaks appearing. Examples of detector-induced artifacts are summarized in Becker and Bergmann [5]. However, the raw measurement of the PToF profile clearly shows that the shape and position of the distribution changes systematically as the count rate is increased. This also shows that the advised count rate for
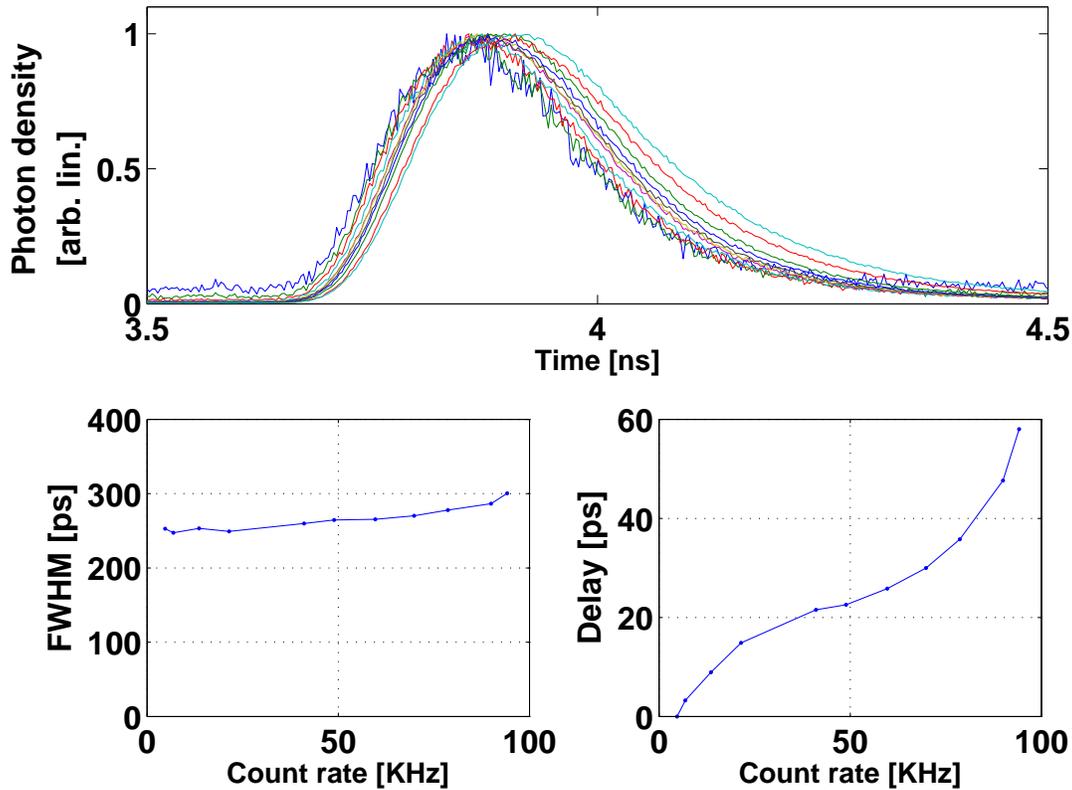
Figure 6. **Top** *Normalized count rate for the PToF distribution of an optical phantom measured at different count rates.* **Bottom** *The measured FWHM of the profiles as a function of the repetition rate and the corresponding temporal delay.*

measurements with the system[1] is too high for obtaining an unperturbed measurement of the PToF distribution. The change in FWHM and delay as a function of count rate shows that the detection of one photon is affected by the previous detection event. An increase in the FWHM can be seen as a reduced likelihood of detecting a photon in the start of the POTF distribution, imposed by the detector setup.

Effect of the light source repetition rate

In a similarly way, the instrument response was investigated as a function of repetition rate. The motivation is that reducing the repetition rate ensures that there is more time between detection events. When the TCP card registers an event on the detector signal, it will not become "armed" until it receives a trigger pulse from the source. Thus if the detector exhibits any afterpulsing effects in-between real detections, this will not affect a new measurement as the TCP card will not register the signal. This is the same effect that the detector is taking into account by using a dead time, and it is also the motivation for operating the SPAD in a gated mode. It was the hoped that a more well-controlled illumination could reduce the non-linearity of the detection which is seen in Figure above.

The measurement is performed on a piece of black paper, which causes a very low additional broadening of the time profile compared to the measurement on the optical phantom presented in Figure 6. The PToF distribution becomes so short, that the detected broadening is given mainly by the detector, this measurement is often referred to as the instrument response function (IRF). The signal was measured at 1510 nm. For this reason, the IRF serves as a extreme measurement and is ideal for quantifying reductions of the measurement artifacts.

The measurements with different repetition rate require different cabling between the SPAD and TCP card to delay the pulses sufficiently to fit a fixed 12.5 ns window for the TCP card. The temporal width of this window is a standard in the laboratory, it matches the period of a laser with a 80 MHz repetition rate and therefore the PTFoF distributions also fits this window. For this reason the absolute position of the profiles on the card vary between measurement with different repetition rate, though a fixed offset of $\sim$ 2.5 ns was used. To make the measurements comparable between repetition rates, the delay was shifted so all measurements were carried out relative to the value at 10 kHz measurement. The measured FWHM values and delays are shown in Figure 7.
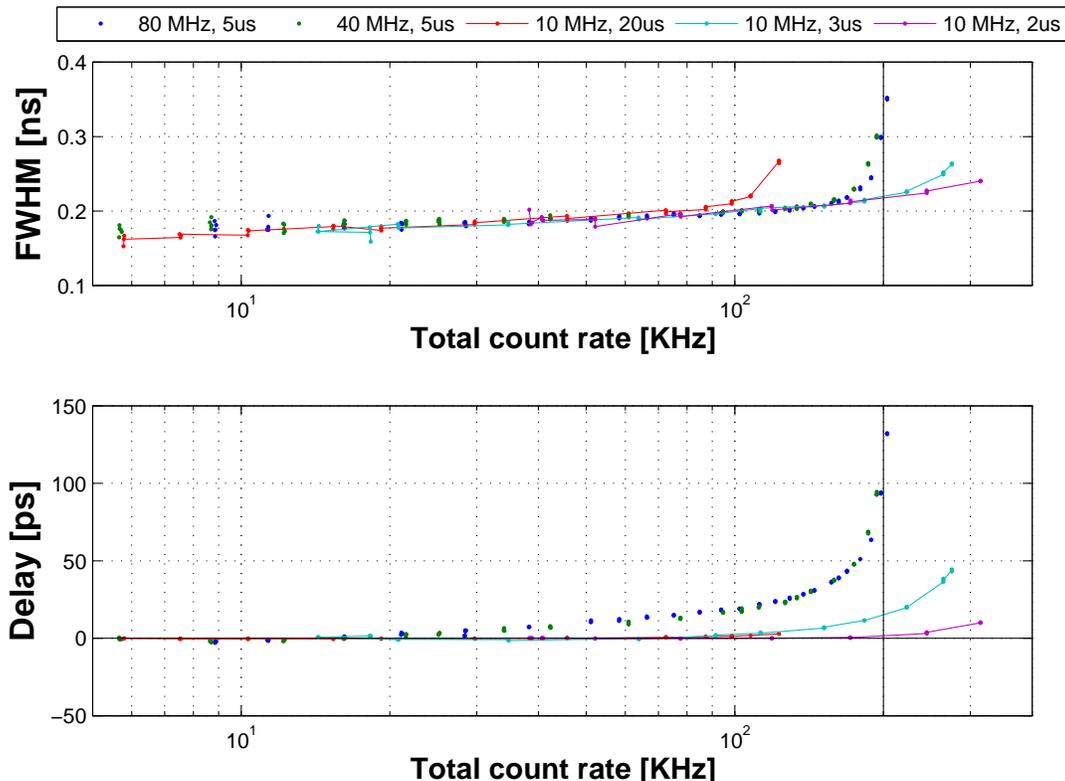
Figure 7. *Instrument characteristics for different combinations of light source repetition rate and dead time, legend notes the repetition rate and dead time.* **Top:** *Absolute value for FWHM vs. count rate.* **Bottom:** *Measured delay relative to the 10 MHz value.*

From Figure 7 it is seen that both the FWHM and the delay diverge towards higher values as the count rate is increased. The results show that the diverges is located around the saturation rate of the detector (defined as the inverse of the dead time). The FWHM value follows the same trend independently of repetition rate and dead time, except in the region close the divergence. Therefore, the only way to minimize this broadening is to reduce the total count rate. However, based on the current results, we do not see a stable regime as such. At the lowest repetition rate the change in signal level is comparable with the variance between measurements. A stable regime may be achieved at lower count rates with increased collection time to provide an adequate signal to noise level.

Concerning the delay time, we again measure a count rate dependent performance, suggesting that the detection is non-linear over the range of count rates we have investigated. The measurements show no significant change upon reducing the repetition rate from 80 MHz to 40 MHz, where the latter was used previously in the literature [18] for PToF spectroscopy. However when operated at 10 MHz, the change in the delay becomes significantly less as a function of the count rate. When combined with a short dead time of 2 - 3 μs, a stable regime is achieved for count rates less than $\sim$ 100 kHz. This shows that the detection artifacts are reduced by using this advanced feature of the light source.

PHOTON TIME-OF-FLIGHT SPECTROSCOPY

To investigate the suitability of the detector for PToF spectroscopy the optical properties of an optical phantom were measured at 1510 nm as a function of count rate. The optical properties are deduced by modeling the temporal profile of the light that has passed though the sample with a analytical expression for diffused light through a finite material slab [14]. The analytical model is convolved with a measured instrument response to account for the temporal broadening of the combined setup. For the analytical model, a refractive index of 1.55 was assumed and the sample was 1.91 mm thick. Examples of the PToF distribution are shown in Figure 8.

From the raw data it is seen that the TOF distribution recorded with a high count rate is delayed, for both cases the model can fit the data, but the fit results in different optical properties. This is a weakness of the technique: the
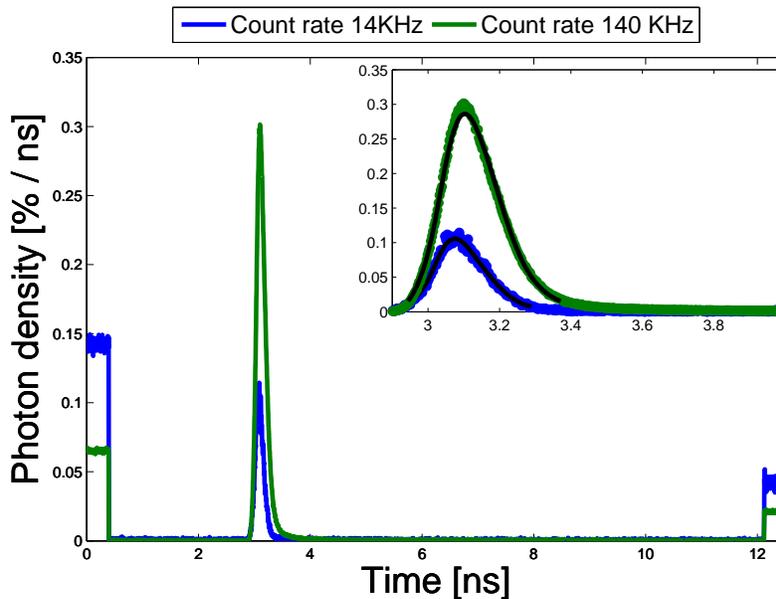
Figure 8. *Example of PToF distributions for the BG36 phantom. The raw data is presented in the main plot, and the graph to the top right shows a zoom into the data with the fitted diffusion expression as black lines.*

optical properties are extracted, with decent fit to the profiles, but all the differences between the measurements is caused by the detector artifacts. Thus the evaluation of the PToF distribution itself does not give a way to quantify or validate the detector performance, it simply gives nice fit to the data with varying optical properties.

To quantify how the count rate affect the deduced optical properties the PToF distribution was measured, and the results are presented in Figure 9. The corresponding reference values for both the delay and the FWHM are given in Figure 10.

The results show systematic decrease in the deduced absorption when the count rate is increased. For scattering, we see a relatively high variance throughout the measurement series, but no systematic change as a function of count rate. This is effectively a trade off between a high noisy value estimation at low count rates and low noise but biased value at higher count rates. The current results indicate that a stable regime has been accomplished at very low count rate, however the measurement exhibits significant noise and may be unsuitable for quantitative spectroscopy due to extensive measurement times to reduce noise.

The associated development of the delay and the FWHM are presented in Figure 10. Both the delay and the FWHM changes when the count rate is increased. As was seen in Figure 7, the change in FWHM is slow and almost linear, and similarly delay is almost constant at low count rates.

A better performance may be achieved by evaluating time of flight profiles on a longer time scale (longer than the 12.5 ns), which also require a reduced repetition rate of the source. The measurement accuracy is, in part, given as the ratio between the temporal width of the instrument response and the measured PToF from the sample. By measuring the temporal profiles on a longer time scale, the detector can be used with a lower QEF which causes a significant drop in the dark count rate of the device. This may provide a easier way for using the device in practice.

CONCLUSION

In this report we have demonstrated a technique for characterization of non-linearities in the response of SPADs for single photon counting in terms of delay and changes in temporal width. These features are useful from an application point of view because they relate directly to the PToF signals that is used for analysis. Using the ID220 it was possible to make measurement of the PToF profile for both optical phantoms and measurement of the systems instrument response function. The results, presented in Figure 6, suggest that the advised collection[17] rate of half the saturation rate (defined by the SPAD dead time) does not give a unbiased estimate of the PToF distribution.

By measuring changes in the instrument response function, it is demonstrated that some of the non-linearities may be minimized by reducing the repetition rate of the light source. Furthermore, it was found that reducing the dead time of the detector removed the systematic change in the pulse delay.
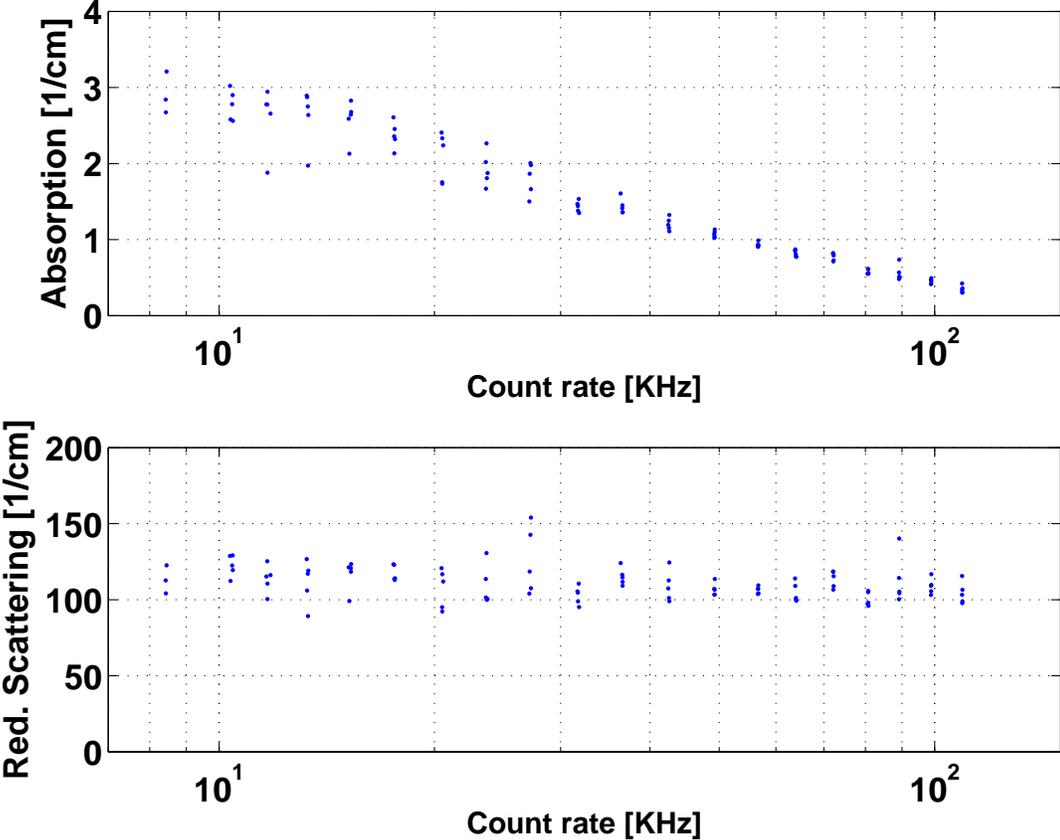
Figure 9. *Deduced optical properties for a BG36 color glass phantom as a function of count rate,* **Top:** *Absorption* **Bottom:** *Reduced scattering*

Based on an improved method of operation, with a low repetition rate and a short dead time, the detector was applied to PToF spectroscopy of tablets composed of BG36 color glass. The deduced optical properties are highly dependent on the count rate during the measurements, which is related to the systematic effects seen on the IRF. However, the results suggest that a stable regime, with high noise of the profiles, was accomplished with the present measurement settings.

In summary the field of single photon counting, and specifically PToF spectroscopy, can benefit from a simple commercially available solution for unbiased estimate of the PToF distribution in the NIR spectral range. We have quantified the detector performance, and demonstrated that artifacts can in part can be eliminated using a commercially available light sources with reduced repetition rate. However, the achieved performance is not sufficient for PToF spectroscopy yet.

The present work have focused on obtaining unperturbed measurements of the PToF distribution. However, it has not addressed how the profiles compared to those obtained with other detector technologies. Future studies may therefore include evaluation of the detectors in the spectral range around 1000 nm where both a PMTs and silicon based SPADs are available as benchmarking instruments.
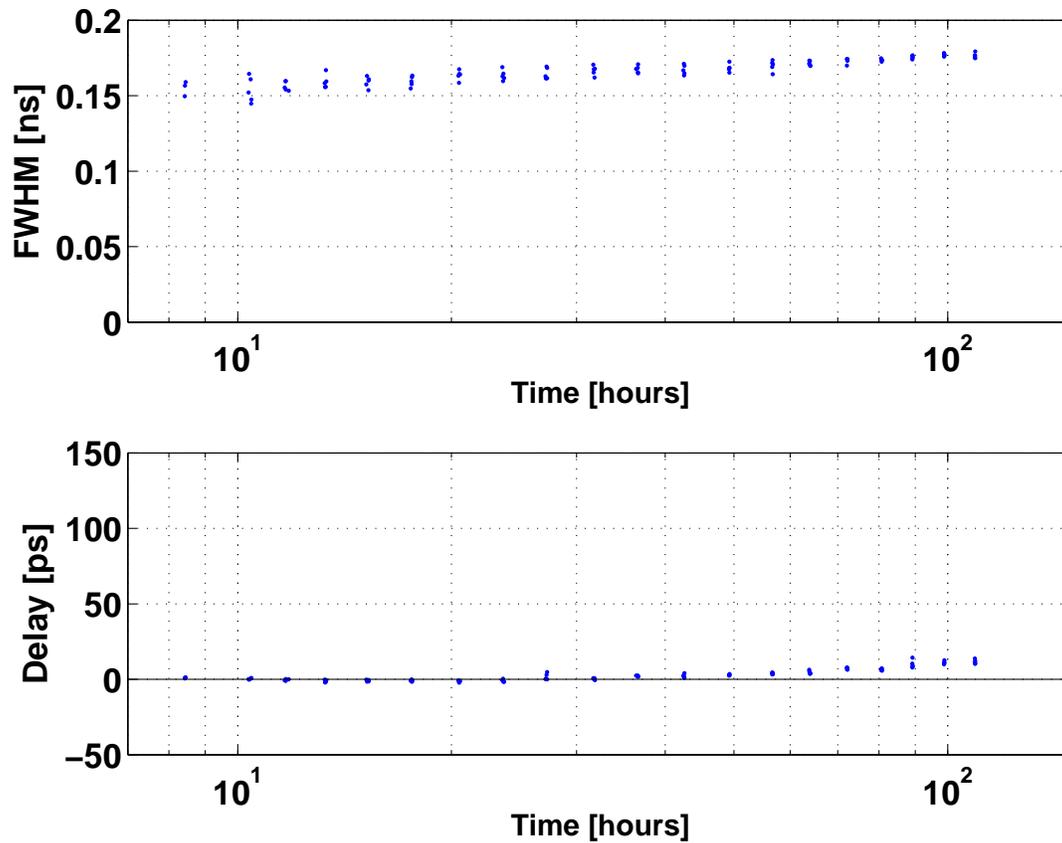
Figure 10. *Pulse characteristics for the series of BG36 measurements presented in figure 9.* **Top:** *full width half maximum* **Bottom:** *temporal delay.*

measurement campaign.

[1] Tcspc at wavelengths from 900 nm to 1700 nm. Technical report, Becker & Hickl GmbH, Nahmitzer Damm 30 , 12277 Berlin, Germany. http://www.becker-hickl.com/pdf/id-220-tcspc-04.pdf.
[2] Christoffer Abrahamsson. *Time-Resolved Spectroscopy for Pharmaceutical Applications.* PhD thesis, Lund Institute of Technology, Department of Physics, 2005.
[3] Erik Alerstam. *Optical spectroscopy of turbid media: time-domain measurements and accelerated Monte Carlo modelling.* PhD thesis, Lund University, 2011.
[4] Ilaria Bargigia, Alberto Tosi, Andrea Bahgat Shehata, Adriano Della Frera, Andrea Farina, Andrea Bassi, Paola Taroni, Alberto Dalla Mora, Franco Zappa, Rinaldo Cubeddu, and Antonio Pifferi. Time-resolved diffuse optical spectroscopy up to 1700 nm by means of a time-gated ingaas/inp single-photon avalanche diode. *Applied Spectroscopy*, 66(8):944–950, Aug 2012.
[5] Wolfgang Becker and Axel Bergmann. *Detectors for High-Speed Photon Counting.* Becker & Hickle.
[6] B. H. Bransden and C. J. Joachain. *Physics of Atoms and Molecules.* Pearson Education Limited, 2003.
[7] JM Dudley, X. Gu, L. Xu, M. Kimmel, E. Zeek, P. O'Shea, R. Trebino, S. Coen, and RS Windeler. Cross-correlation frequency resolved optical gating analysis of broadband continuum generation in photonic crystal fiber: simulations and experiments. *Optics Express*, 10(21):1215–1221, 2002.
[8] G V Dyatlov, K V Gilev, M A Yurkin, and V P Maltsev. An optimization method with precomputed starting points for solving the inverse mie problem. *Inverse Problems*, 28(4):045012, 2012.
[9] Matthew W. Fishburn and Edoardo Charbon. Monolithic single-photon avalanche diodes: Spads. *Springer Series in Optical Sciences*, 160:123–157, 2011.
[10] Mark A. Itzler, Xudong Jiang, and Mark Entwistle. Power law temporal dependence of ingaas/inp spad afterpulsing. *Journal of Modern Optics*, 59(17):1472–1480, 2012.

[11] X. Li, ZG Chen, A. Taflove, and V. Backman. Epuiphase-sphere approximation for analysis of light scattering by arbitrarily shaped nonspherical particles. *Applied Optics*, 43(23):4497–4505, 2004.

[12] Zhiwen Lu, Wenlu Sun, J. Campbell, Xudong Jiang, and M.A. Itzler. Single photon detection with sine gated dual ingaas/inp avalanche diodes. In *Photonics Conference (IPC), 2012 IEEE*, pages 98–99, 2012.

[13] Tommaso Lunghi, Claudio Barreiro, Olivier Guinnard, Raphael Houlmann, Xudong Jiang, Mark A. Itzler, and Hugo Zbinden. Free-running single-photon detection based on a negative feedback ingaas apd. *Journal of Modern Optics*, 59(17):1481–1488, 2012.

[14] Fabrizio Martelli, Daniele Contini, Adriana Taddeucci, and Giovanni Zaccanti. Photon migration through a turbid slab described by a model based on diffusion approximation. ii. comparison with Monte Carlo results. *Applied Optics*, 36(19):4600–4612, Jul 1997.

[15] Fabrizio Martelli, Samuele Del Bianco, Andrea Ismaelli, and Giovanni Zaccanti. *Light propagation through biological tissue and other diffusive media: theory, solutions, and software*. SPIE Press Bellingham, 2010.

[16] N. Namekata and Shuichiro Inoue. Afterpulsing-free 80mhz single-photon detection at 1550 nm using an ingaas/inp avalanche photodiode operated with sinusoidal gating. In *Lasers and Electro-Optics, 2007 and the International Quantum Electronics Conference. CLEOE-IQEC 2007. European Conference on*, pages 1–1, 2007.

[17] Described in [1].

[18] Antonio Pifferi, Alessandro Torricelli, Lorenzo Spinelli, Davide Contini, Rinaldo Cubeddu, Fabrizio Martelli, Giovanni Zaccanti, Alberto Tosi, Alberto Dalla Mora, Franco Zappa, and Sergio Cova. Time-resolved diffuse reflectance using small source-detector separation and fast single-photon gating. *Physical Review Letters*, 100(13):138101, Mar 2008.

[19] Tomas Svensson. *Pharmaceutical and Biomedical Applications of Spectroscopy in the Photon Migration Regime*. PhD thesis, Lund University, 2008.

[20] Xin Wang, Pogue, Shudong Jiang, Xiaomei Song, Paulsen, Kogel, Poplack, and Wells. Approximation of mie scattering parameters in near-infrared tomography of normal breast tissue in vivo. *Journal of Biomedical Optics*, 10(5):51704–1–8, 2005.

[21] Zhizhong Yan, Deny R. Hamel, Aimee K. Heinrichs, Xudong Jiang, Mark A. Itzler, and Thomas Jennewein. An ultra low noise telecom wavelength free running single photon detector using negative feedback avalanche diode. *Review of Scientific Instruments*, 83(7):–, 2012.